

Multi-Resonator-Assisted Multi-Qubit Resetting in a Network

Xian-Peng Zhang^{1,2}, Li-Tuo Shen¹, Zhang-Qi Yin³, Luyan Sun³, Huai-Zhi Wu¹, and Zhen-Biao Yang^{1*}

1.Department of Physics, Fuzhou University, Fuzhou, 350116, P. R. China

2.Department of Physics, National Tsing Hua University, Hsinchu, 300, Taiwan and

3.Center for Quantum Information, Institute for Interdisciplinary Information Sciences, Tsinghua University, Beijing 100084, P. R. China

We propose a quantum bath engineering method for the initialization of arbitrary number of flux-tunable transmon qubits with a multi-resonator circuit quantum electrodynamics (QED) architecture. Through the application of the microwave drives, we can prepare any number of qubits distributed among the network into arbitrary initial states (on the Bloch sphere surface). Taking into account the practically experimental parameters, we verify that the initialization process could be achieved in $1\mu\text{s}$ with the fidelity in excess of 99%. Moreover, due to the special structure of the circuit network, the initialization efficiency is independent on the number of (ideal, provided) qubits, as only a definite number of bosonic modes are involved in despite of the increasing number of the qubits to be initialized.

PACS numbers:

The turn of this century has witnessed so many advances in theoretical and experimental frontiers of quantum information processing, including quantum computation [1, 2], simulation [3–5] as well as communication [6, 7], with an outlook that many intellectual breakthroughs and technical innovations are still to be made in the future [8–10]. The physical realization of quantum computing generally requires the ability to initialize qubit to arbitrary superposition of computational basis states [11]. Determinately and quickly initializing qubit into any well-defined state provides a convenient avenue for an error-corrected information processor [12–14], as well as for quantum memories [15–17].

The traditional route to generate coherence and entanglement relies on minimizing coupling to a dissipative bath. Alternatively, demanding control over the coupling in engineer is replaced by a relatively open environment that allows dissipation to actually assist the generation of coherence and entanglement [18–20]. Cavity- or resonator-assisted cooling, which dissipates the kinetic energy in a dissipative environment created by cavity or resonator photon loss, has become eye-catching in artificial atoms [21–24], genuine atoms [25, 26], spins [27, 28], and mechanical objects [29–31]. A paradigmatic example is quantum state engineering of a single qubit in a quantum bath, where dissipation may be engineered to relax the system towards any arbitrary states (corresponding to points on the Bloch sphere surface) [22]. Recently, it was demonstrated that cavity-assisted cooling of ensemble spin and artificial atom systems can be implemented on a timescale about microseconds [22, 28]. Resonator-assisted quantum bath engineering may be used to prepare the superconducting flux qubit into any orbital state of the Bloch sphere surface with a controllable phase factor [24]. However, these gratifying schemes all focus on

a single qubit. In quantum computation, the operation of logic gates requires direct or indirect coupling between qubits. During the process, one of the most critical challenges is how to effectively initialize designated qubits while with the other qubits unaffected [11], especially in such an always-connected circuit network [10].

We propose here an effective quantum bath engineering method for initializing arbitrary multiple flux-tunable transmon qubits with a multi-resonator circuit quantum electrodynamics (QED) architecture. In this work, independent, rapid and precise control over the internal state of the flux-tunable transmon qubit, allows us to prepare arbitrary qubits into any well-defined states for random initial states. The Markovian master equation describing the quantum circuit has been solved in the presence of the corresponding (say, to qubits) adjustable microwave drives. Our calculations verified by Monte-Carlo simulation indicate that arbitrary number of qubits are able to be simultaneously prepared into redefined ground states for random initial states with short polarization time in the 0.2-0.8 μs range for the experimentally feasible sample parameters, which is significantly shorter than the intrinsic energy relaxation time for the superconducting flux qubit in the 6-20 μs range [32, 33]. Our numerical calculations certify that such a method is tolerable of considerable fluctuation of system's parameters.

The computational basis states of our circuits are realized using the two lowest energy levels, $|0\rangle$ and $|1\rangle$, of the flux-tunable transmon qubit [34]. As shown in FIG. 1(a), a transmon-type qubit capacitively coupled to two of its adjacent resonators constructs the scalable structural block, N such blocks capacitively coupled to each other form the multi-resonator multi-qubit circuit QED network. Qubits interact through two strongly coupled resonators, served as a Purcell filter, to suppress the off-resonant interactions [35]. This multi-resonator multi-qubit circuit QED architecture is feasible for the current experiment technology [36]. In the presence of N independently adjustable microwave drives, acting one-

*Electronic address: zbyang@fzu.edu.cn

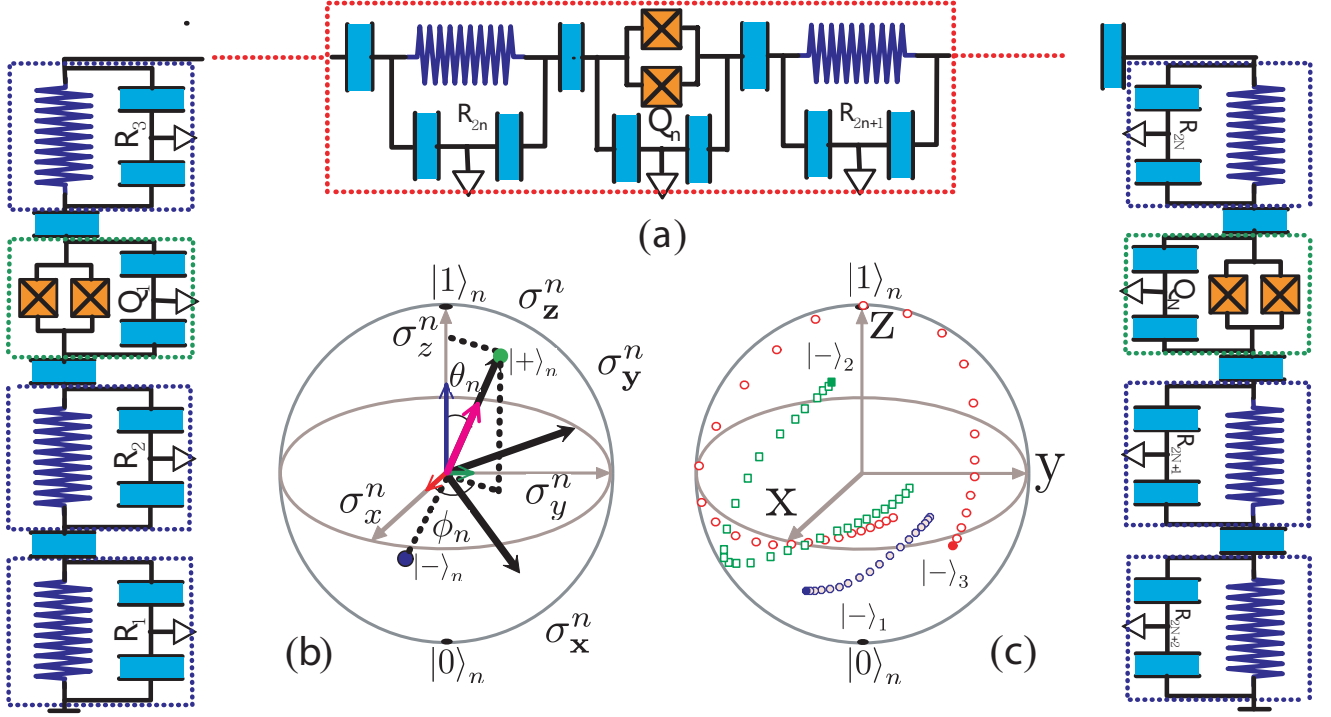


FIG. 1: (a) Schematic diagram of the multi-resonator multi-qubit circuit QED architecture: a transmon-type qubit (surrounded by green dotted rectangular) capacitively coupled to two of its adjacent resonators (surrounded by blue dotted rectangular) constructing the scalable structural block (surrounded by red dotted rectangular), N such blocks capacitively coupled to each other form the multi-resonator multi-qubit circuit QED network. (b) Rotation of Pauli operators. Assume that the n th qubit should be initialized into the state $|- \rangle_n = \cos(\frac{\theta_n}{2})|0\rangle + e^{i\phi_n} \sin(\frac{\theta_n}{2})|1\rangle$, which is the eigenstate of the redefined Pauli operator $\sigma_z^n = -\sin\theta_n \cos\phi_n \sigma_x + \sin\theta_n \sin\phi_n \sigma_y + \cos\theta_n \sigma_z$ with eigenvalue -1 , i.e., ground state. This Pauli operator σ_z^n (pink arrow) can be obtained by an around- z -axis rotation with angle $\phi - R_z(\phi)$ followed by an around- y -axis rotation with angle $\theta - R_y(\theta)$. The detuning of the drive (blue arrow), the real part (red arrow) and imaginary part (green arrow) of the Rabi frequency should be adjusted to satisfy Eq. (3), which gives clear direction to polarization process. (c) Drive of low-temperature quantum bath. Effective initialization happens, when the spectrums of the microwave resonator, the filter-filter coupling and the effective Rabi frequency match, i.e., $\delta\omega - v - 2\Omega = 0$. Quantum bath engineering created by the resonator photon shot noise drives each qubit to its target states $|- \rangle_n$ for random initial states. Here we set $N = 3$.

to-one on N qubits, oscillation between energy levels $|0\rangle$ and $|1\rangle$ of each qubit with regulable frequency ω_n is induced near resonance. We can write the Hamiltonian for the whole quantum circuit within the standard rotating wave approximation (RWA) as well as in the rotating frame $R_1 = \sum_{m=1}^{2N+2} \varpi_L a_m^+ a_m + \sum_{n=1}^N \varpi_L \sigma_z^n / 2$ as ($\hbar = 1$ is assumed)

$$\begin{aligned}
 H_1 = & \sum_{m=1}^{2N+2} \delta\omega a_m^+ a_m + \sum_{n=1}^{N+1} v a_{2n-1}^+ a_{2n}^+ + v a_{2n-1}^+ a_{2n} \\
 & + \sum_{n=1}^N \text{Re}(\Omega_n) \sigma_x^n + \text{Im}(\Omega_n) \sigma_y^n + \delta\varpi_n \sigma_z^n / 2 \\
 & + \sum_{n=1}^N g(a_{2n}^+ + a_{2n+1}^+) \sigma_-^n + g(a_{2n} + a_{2n+1}) \sigma_+^n \quad (1)
 \end{aligned}$$

with $\delta\omega = \omega_c - \varpi_L$ and $\delta\varpi_n = \omega_n - \varpi_L$, where a_m (a_m^+) is the annihilation (creation) operator of the m th resonator with the frequency ω_c , σ_+^n (σ_-^n) and σ_j^n are the raising (lowering) and j -direction ($j = x, y, z$) Pauli operators

of the n th qubit with the frequency ϖ_L , Ω_n is the Rabi frequency of the drive acting on the n th qubit, v is the filter-filter coupling and g is the qubit-filter interaction. Our design concept is illustrated in FIG. 1(b)-(c). Firstly, we rotate the Pauli operators of each qubit, as depicted in FIG. 1(b), which makes the low-eigenvalue eigenstate of the rotated Pauli operator to be the target state of the n th qubit. Secondly, the photon-loss-assisted driving could stabilize each qubit to its redefined ground state, i.e., the required state, as depicted in FIG. 1(c). For the n th qubit, any specified point on the Bloch sphere surface $|- \rangle_n = \cos(\frac{\theta_n}{2})|0\rangle + e^{i\phi_n} \sin(\frac{\theta_n}{2})|1\rangle$ with $\theta_n \in [0, \pi]$ and $\phi_n \in [0, 2\pi)$, must be the eigenstate of the Pauli operator after rotation $\sigma_z^n = -\sin\theta_n \cos\phi_n \sigma_x + \sin\theta_n \sin\phi_n \sigma_y + \cos\theta_n \sigma_z$ with eigenvalue -1 , i.e., ground state. This rotation is able to be realized by an around- z -axis rotation with angle ϕ_n followed by an around- y -axis rotation with angle θ_n (As depicted in FIG. 1(b), where the bold subscripts $\mathbf{x}, \mathbf{y}, \mathbf{z}$ indicate the space basics after rotation). By weakly coupling each qubit to adjacent resonators with capacitance and by employing a microwave drive

that is near resonance with the qubit transition, the engineered low-temperature quantum bath could drive each flux-tunable transmon qubit to its ground state $|- \rangle_n$.

In analogy to resonator-assisted quantum bath engineering [24], we here introduce a rotating transformation \mathbf{R}^n of Pauli operators for each qubit to investigate the polarization efficiency of the arbitrary direction

$$\begin{bmatrix} \sigma_x^n \\ \sigma_y^n \\ \sigma_z^n \end{bmatrix} = \begin{bmatrix} \cos \theta_n \cos \phi_n & -\cos \theta_n \sin \phi_n & \sin \theta_n \\ \sin \phi_n & \cos \phi_n & 0 \\ -\sin \theta_n \cos \phi_n & \sin \theta_n \sin \phi_n & \cos \theta_n \end{bmatrix} \begin{bmatrix} \sigma_x^n \\ \sigma_y^n \\ \sigma_z^n \end{bmatrix}, \quad (2)$$

where the rotation angles θ_n and ϕ_n are determined by the Rabi frequency and the detuning of the n th drive field with

$$-\frac{\text{Re}(\Omega_n)}{\sin \theta_n \cos \phi_n} = \frac{\text{Im}(\Omega_n)}{\sin \theta_n \sin \phi_n} = \frac{\delta \varpi_n}{2 \cos \theta_n}. \quad (3)$$

We can define this ratio as an effective Rabi frequency

$$\bar{\Omega} \equiv [|\Omega_n|^2 + |\delta \varpi_n|^2/4]^{1/2}, \quad (4)$$

where we have removed the n -dependence of that by adjusting Ω_n and $\delta \varpi_n$ for simplicity.

In the rotating frame of $R_2 = \sum_{n=1}^N \bar{\Omega} \sigma_z^n + \sum_{m=1}^{2N+2} \delta \omega a_m^+ a_m + \sum_{n=1}^{N+1} v(a_{2n-1} a_{2n}^+ + a_{2n-1}^+ a_{2n})$, the Hamiltonian generates six modes $M(m, n)$ ($m = \pm 1, n = 0, \pm 1$) with frequencies $\omega_{mn} = \delta \omega + mv + 2n\bar{\Omega}$. We here make a brief summation of the functions of these six modes. There is no preference in the σ_z^n direction for the dynamics of modes $M(m, 0)$ at the thermal equilibrium, while those of modes $M(m, \pm 1)$ would drive the qubit to the $\langle \sigma_z^n \rangle = \pm 1$ states, respectively [24, 28]. Therefore, modes $M(m, -1)$ must dominate our polarization process. Here we prefer the mode $M(-1, -1)$ [37]. We may set $\Delta = \delta \omega - v - 2\bar{\Omega}$ to be close to zero, choose the strong enough filter-filter coupling, and make the effective Rabi frequency satisfy $2\bar{\Omega}, 2v \gg \Delta$, so that other high-frequency modes $M(m, n)$ separate well from mode $M(-1, -1)$. In the interaction frame of R_2 , the Hamiltonian reduces into $H_I(t) = \sum_{n=1}^N H_n(t)$ with

$$H_n = \sum_{m=2n-1}^{2n+2} \frac{g}{4} (\cos \theta_n + 1) e^{i(\Delta t + \phi_n)} a_m^+ \sigma_-^n(\mathbf{z}) + H.c.. \quad (5)$$

where we use again RWA in the parameter regime where $2\bar{\Omega}, 2v$ are large compared to the dissipation rate of the resonator, κ , and the qubit-filter coupling g , i.e., $2\bar{\Omega}, 2v \gg \kappa, g$.

We now move on to study the polarization efficiency of each qubit dominated by the mode $M(-1, -1)$, i.e., $\Delta \rightarrow 0$. The evolution of the multi-resonator multi-qubit circuit in an open environment can be modeled by the Lindblad master equation

$$\frac{d}{dt} \rho(t) = L[H_I(t)]\rho(t) + D_c \rho(t), \quad (6)$$

with

$$D_c = \sum_{m=1}^{2N+2} \frac{\kappa}{2} ((1 + \bar{n})D[a_m] + \bar{n}D[a_m^+]). \quad (7)$$

where the qubit dissipation is at the moment left out of consideration, L is the superoperator $L[H_I(t)]\rho(t) = -i[H_I(t), \rho]$ describing the unitary evolution under the domination of H_I , D_c is a dissipator representing the dissipative environment created by resonator photon loss, $D[O]\rho = 2O\rho O^\dagger - \{O^\dagger O, \rho\}$, $\bar{n}_m = \text{tr}_c[a_m^+ a_m \rho_{eq}] = 1/(e^{\omega_c/k_B T_c} - 1)$ is the expectation value of the photon number operator at equilibrium associated with the temperature of the resonators, T_c , and the Boltzmann constant k_B .

The reduced dynamics of flux-tunable transmon qubits in the interaction frame of the dissipator is given by the 2nd order time-convolutionless master equation (See Appendix B):

$$\dot{\varrho}(t) = - \int_0^t d\tau e^{-\kappa\tau/2} \text{tr}_c[[H_I(t), [H_I(t-\tau), \varrho(t) \otimes \rho_{eq}]]]. \quad (8)$$

If the condition in Eq. (3) is satisfied, the n th qubit with the target state characterized by the specified point on the Bloch sphere surface (θ_n, ϕ_n) can be effectively polarized, when the spectrums of the microwave resonator, the filter-filter coupling and the effective Rabi frequency match, i.e., $\Delta \rightarrow 0$. Then the effective polarization rate of each qubit becomes (See Appendix B):

$$\Gamma_n = \frac{(1 + \cos \theta_n)^2 g^2}{1 + 4(\Delta/\kappa)^2 \kappa}. \quad (9)$$

With the definition of $\vec{P}_{\sigma_z^n}(t) = [P_{-1}(t), P_1(t)]^T$, where $P_{\sigma_z^n}(t) = \langle \sigma_z^n | \varrho(t) | \sigma_z^n \rangle$ ($\sigma_z^n = \pm 1$) is the expectation value of the projection operator $|\sigma_z^n\rangle \langle \sigma_z^n|$ at an arbitrary time t , the Lindblad master equation will reduce to a rate equation for the state populations of each qubit:

$$\frac{d}{dt} \vec{P}_{\sigma_z^n}(t) = \Gamma_n \mathbf{M} \vec{P}_{\sigma_z^n}(t), \quad (10)$$

with

$$\mathbf{M} = \begin{bmatrix} -\bar{n} & \bar{n} + 1 \\ \bar{n} & -(\bar{n} + 1) \end{bmatrix}. \quad (11)$$

In equilibrium, the steady state of the flux-tunable transmon qubit satisfies $\partial_t \vec{P}_{\sigma_z^n}(t) = 0$ and the expectation value of the operator σ_z^n for the equilibrium state is

$$\langle \sigma_z^n \rangle_{eq} = \frac{e^{-\omega_c/k_B T_c} - 1}{e^{-\omega_c/k_B T_c} + 1}. \quad (12)$$

In the ideal case where all resonators are cooled to their ground states, i.e., vacuum states ($T_c \rightarrow 0$), the final expectation value is approximately $\langle \sigma_z^n \rangle_{eq} \simeq -1$.

The separability of rate equation (10) for each qubit makes it easy for us to simulate the gratifying results. For the n th qubit initially taken to be maximally mixed in the basis, i.e., $P_{\sigma_z^n}(0) = 1/2$ ($\sigma_z^n = \pm 1$), the evolutions of the simulated expectation values $\langle \sigma_z^n \rangle$ for different temperatures $T_c = 0.0, 0.3, 0.4, 0.5$ K are shown in FIG. 2 with equilibrium expectation values $-1.000, -0.995, -0.979, -0.948$, respectively. The evolution of the simulated expectation value $\langle \sigma_z^m \rangle$ for temperature $T_c \leq 0.3$ K (within which the thermodynamics effect may not be observed [32, 33]) may be fitted to an exponential function to derive an effective polarization time constant, T_n . A fit to a model given by $\langle \sigma_z^n \rangle = \exp(-t/T_n) - 1$ yields the parameter

$$T_n \simeq \frac{1}{\Gamma_n} = \frac{1 + 4(\Delta/\kappa)^2 \kappa}{(1 + \cos \theta_n)^2 g^2}. \quad (13)$$

We find that the resetting efficiency is independent on the number of qubits. Inset of FIG. 2 depicts the effective dissipation rate versus the dimensionless parameters Δ/κ and θ_n in the units of g^2/κ . Apparently, the polarization time increases rapidly, when the Stokes photons are off-resonant with the resonator and the condition $\Delta \gg \kappa$ is satisfied. And the most efficient polarization happens in z direction with the effective dissipation rate $\Gamma_n = 4g^2/\kappa$ ($\theta_n = 0, \Delta = 0$).

Here we consider the experimentally feasible parameters: $v/2\pi = 100$ MHz, $\bar{\Omega}/2\pi = 100$ MHz, $\omega_L/2\pi = 5.7$ GHz and $\omega_c/2\pi = 6$ GHz. If we want to initialize the n th qubit into the state $|- \rangle_n = \cos(\frac{\theta_n}{2})|0\rangle + e^{i\phi_n} \sin(\frac{\theta_n}{2})|1\rangle$, the qubit frequency should be set to be $\omega_n = \omega_L + 2\bar{\Omega} \cos \theta_n$, and the microwave drive acting on this qubit should be adjusted with $[\text{Re}(\Omega_n), \text{Im}(\Omega_n), \delta\varpi_n/2] = [-\bar{\Omega} \sin \theta_n \cos \phi_n, \bar{\Omega} \sin \theta_n \sin \phi_n, \bar{\Omega} \cos \theta_n]$. In such a case, the polarization time, T_n , of each qubit is of the range of $0.2 - 0.8 \mu\text{s}$ in the parameter regime $(g, \kappa)/2\pi = (2, 20)$ MHz, which is significantly shorter than the intrinsic energy relaxation time for the superconducting flux qubit in the $6-20 \mu\text{s}$ range [32, 33].

Assume that the quantum circuit has three qubits ($N = 3$) and should be initialized into $[\langle \sigma_x^1 \rangle, \langle \sigma_y^1 \rangle, \langle \sigma_z^1 \rangle] = [-1, -1, -1]$ state. For the initial state $[\langle \sigma_y^1 \rangle, \langle \sigma_z^2 \rangle, \langle \sigma_z^3 \rangle] = [1, 1, 1]$, a Monte Carlo method is used to simulate the Lindblad master equation of the interaction Hamiltonian H_1 , based on Quantum Toolbox in Python [38, 39]. FIG. 3(a) describes the evolutions of the expectation values $\langle \sigma_z^n \rangle$ of the qubits in the parameter regime $(g, \kappa)/2\pi = (2, 20)$ MHz. Apparently, it is consistent with the inset of FIG. 3(a), which shows the evolutions of the expectation values $\langle \sigma_z^n \rangle$ of the qubits for the rate equation (10). As shown in FIG. 3(a), all qubits are able to reach a quite high reliability with the final expectation values $[\langle \sigma_x^1 \rangle, \langle \sigma_y^2 \rangle, \langle \sigma_z^3 \rangle] \approx [-0.9998, -0.9997, -1.0000]$. We can obviously observe that the speed of the simulated expectation value $\langle \sigma_z^3 \rangle$ (approaching -1) is four times as fast as those of the simulated expectation values $\langle \sigma_x^1 \rangle$ and $\langle \sigma_y^2 \rangle$, which validates the analytical derivation

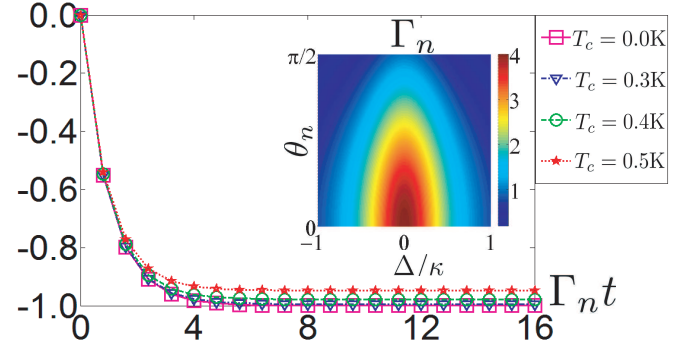


FIG. 2: The evolutions of the simulated expectation values $\langle \sigma_z^n \rangle$ for different temperatures $T_c = 0.0$ K (Square), $T_c = 0.3$ K (Triangle), $T_c = 0.4$ K (Circle) and $T_c = 0.5$ K (Pentagram), where time axis is scaled by the effective dissipation rate, Γ_n , of the n th qubit. Inset is the effective dissipation rate in the unit of g^2/κ versus the dimensionless parameters Δ/κ and θ_n . The most efficient polarization happens in z -direction with the effective dissipation rate $\Gamma_n = 4g^2/\kappa$ ($\cos \theta_n = 1, \Delta = 0$), where the time corresponding to $\Gamma_n t = 16$ is $3.2 \mu\text{s}$ in the parameter regime $(g, \kappa)/2\pi = (2, 20)$ MHz. Parameter: $v/2\pi = 100$ MHz, $\bar{\Omega}/2\pi = 100$ MHz, $\omega_L/2\pi = 5.7$ GHz, $\omega_c/2\pi = 6$ GHz, $\Omega_n = \bar{\Omega} e^{i(\pi - \phi_n)}$ and $\omega_n = \omega_L + 2\bar{\Omega} \cos \theta_n$.

of the effective θ_n -dependent dissipation rate (9) with $\Gamma_3 = 4\Gamma_1 = 4\Gamma_2$.

The influences of the fluctuations of parameters Ω_n and $\delta\varpi_n$ have been previously studied and are normally small enough to be neglected [24]. Simulation results show that the considerable fluctuations of parameters κ and g are also allowed. The polarization efficiency can be improved when we make an optimization of the parameters $(g, \kappa)/2\pi = (15, 10)$ MHz, as shown in FIG. 3(b), where all transmon-type qubits are almost completely driven into their target states after $0.32 \mu\text{s}$ polarization process with $[\langle \sigma_x^1 \rangle, \langle \sigma_y^2 \rangle, \langle \sigma_z^3 \rangle] \approx [-0.998, -0.998, -1.000]$. This significant improvement over previous works opens the way to multi-resonator multi-qubit network quantum protocols across a range of quantum algorithm, photonic memory, and nascent quantum simulation.

The qubit dissipation will make a disturbance on the equilibrium state and should be considered before it comes to the conclusion. In the presence of qubit decay and qubit dephasing, the Lindblad master equation of the quantum system is

$$\begin{aligned} \frac{d}{dt} \rho(t) = & L[H_1] \rho(t) + D_c \rho(t) \\ & + \sum_{n=1}^N \frac{1}{T_\theta} D[\sigma_-^{(z)}] \rho(t) + \frac{1}{2T_\phi} D[\sigma_z^{(z)}] \rho(t), \end{aligned} \quad (14)$$

where $1/T_\theta$ and $1/T_\phi$ are the rates for qubit decay and qubit dephasing, respectively. The evolutions of the expectation values $\langle \sigma_j^n \rangle$, with the experimentally available parameters $(T_\theta, T_\phi) = (20, 10) \mu\text{s}$ [33], are simulated for the master equation in Eq. (14). We note that a quite

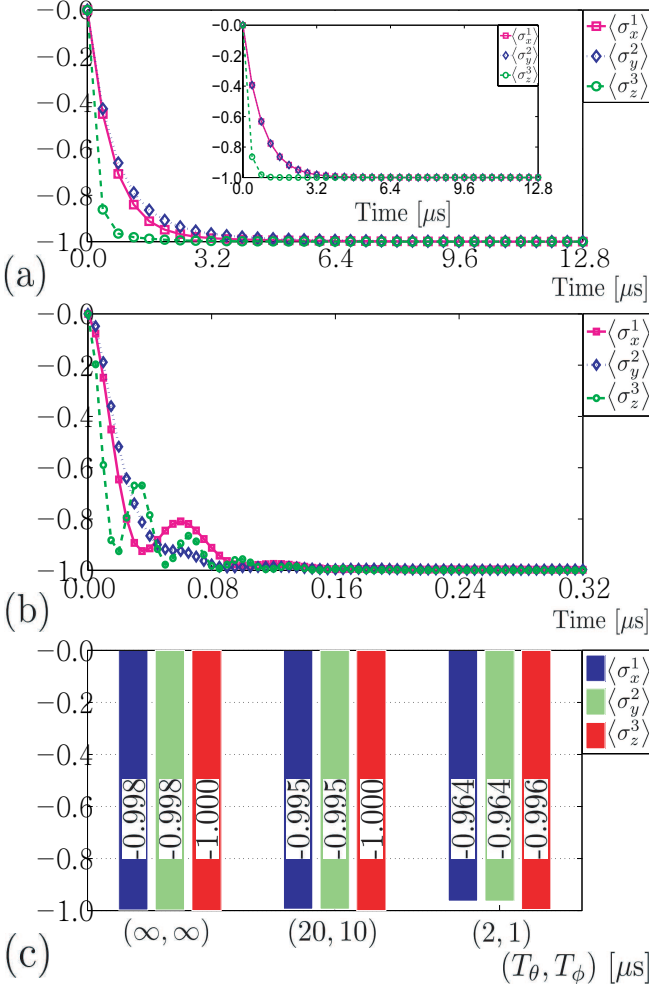


FIG. 3: (a)-(b) The evolutions of the simulated expectation values $\langle \sigma_z^n \rangle$ of three qubits with the Lindblad master equation for the parameter regimes (a) $(g, \kappa)/2\pi = (2, 20)$ MHz and (b) $(g, \kappa)/2\pi = (15, 10)$ MHz. Inset of FIG. 3(a) describes the evolutions of the expectation values $\langle \sigma_z^n \rangle$ of 3 qubits for the rate equation (10). (c) The final expectation values $\langle \sigma_z^n \rangle$ of the master equation (14) in the parameter regime $(g, \kappa)/2\pi = (15, 10)$ MHz for three different sets of qubit dissipation rates $(1/T_\theta, 1/T_\phi)$. Parameter: $v/2\pi = 100$ MHz, $\Omega_1/2\pi = 100$ MHz, $\Omega_2/2\pi = 100i$ MHz, $\Omega_3/2\pi = 0$ MHz, $\omega_L/2\pi = 5.7$ GHz, $\omega_1/2\pi = 5.7$ GHz, $\omega_2/2\pi = 5.7$ GHz, $\omega_3/2\pi = 5.9$ GHz and $\omega_c/2\pi = 6$ GHz.

high reliability can be obtained with the final expectation values $[\langle \sigma_x^1 \rangle, \langle \sigma_y^2 \rangle, \langle \sigma_z^3 \rangle] \approx [-0.995, -0.995, -1.000]$, as shown in FIG. 3(c). This means that the proposed scheme is in principle feasible with the presently experimental sample parameters.

In conclusion, we have demonstrated a quantum bath engineering method for the initialization of arbitrary number of flux-tunable transmon qubits with a multi-resonator circuit QED architecture. Precise, rapid and independent control over the internal states of transmon-type qubits, allows us to achieve flexible resetting for any designated qubits in an always-connected circuit network.

This work is supported by the National Natural Science Foundation of China under Grants No.11405031, No.11305037, No.11374054 and No.11347114, the Major State Basic Research Development Program of China Under Grant No.2012CB921601, the Natural Science Foundation of Fujian Province under Grant No.2014J05005, and the fund from Fuzhou University. Z.-Q.Y. is supported by the National Natural Science Foundation of China under Grants No.61435007 and No.11474177. L.-Y.S. is supported by the National Natural Science Foundation of China under Grant No.11474177 and the 1000 Youth Fellowship program in China.

Appendix: Derivation of Markovian Master Equation and Analysis of Approximations

A. System Hamiltonian

Here we consider the microwave drive acting on each flux-tunable transmon qubit is nearly resonant with the corresponding qubit frequency ω_n ($n = 1 \sim N$), the composite Hamiltonian of the multi-resonator multi-qubit network for the superconducting circuit is $H = H_0 + H_r + H_d + H_h$ with ($\hbar = 1$ is assumed)

$$H_0 = \sum_{m=1}^{2N+2} \omega_c a_m^\dagger a_m + \sum_{n=1}^N \frac{\omega_n}{2} \sigma_z^n, \quad (\text{A.1})$$

$$H_r = \sum_{n=1}^N g a_{2n} \sigma_x^n + g a_{2n+1} \sigma_x^n + H.c., \quad (\text{A.2})$$

$$H_d = \sum_{n=1}^N \Omega_n \sigma_-^n e^{i\omega_L t} + \tilde{\Omega}_n \sigma_-^n e^{-i\omega_L t} + H.c., \quad (\text{A.3})$$

$$H_h = \sum_{n=1}^{N+1} v a_{2n-1} a_{2n}^\dagger + v a_{2n-1}^\dagger a_{2n}, \quad (\text{A.4})$$

where a_m (a_m^\dagger) is the annihilation (creation) operator of the m th resonator with the frequency ω_c , Ω_n and $\tilde{\Omega}_n$ are the Rabi and the counter-rotating Rabi frequencies of the drive acting on the n th qubit, σ_+ (σ_-) and σ_j ($j = x, y, z$) are the raising (lowering) and j -direction ($j = x, y, z$) Pauli operators of the n th qubit with the frequency ω_L , v is the filter-filter coupling and g is the qubit-filter coupling. In rotating frame defined by $R_1 = \sum_{m=1}^{2N+2} \omega_L a_m^\dagger a_m + \sum_{n=1}^N \omega_L \sigma_z^n / 2$, the system Hamiltonian becomes

$$\begin{aligned} H_1 = & \sum_{m=1}^{2N+2} \delta \omega a_m^\dagger a_m + \sum_{n=1}^{N+1} v a_{2n-1} a_{2n}^\dagger + v a_{2n-1}^\dagger a_{2n} \\ & + \sum_{n=1}^N \text{Re}(\Omega_n) \sigma_x^n + \text{Im}(\Omega_n) \sigma_y^n + \delta \omega_n \sigma_z^n / 2 \\ & + \sum_{n=1}^N g (a_{2n}^\dagger + a_{2n+1}^\dagger) \sigma_-^n + g (a_{2n} + a_{2n+1}) \sigma_+^n \end{aligned} \quad (\text{A.5})$$

with $\delta\omega = \omega_c - \omega_L$ and $\delta\varpi_n = \omega_n - \omega_L$, where we have made the standard rotating wave approximation (RWA) to remove any time-dependent terms of the Hamiltonian, in the parameter regime $\omega_c, \omega_L, \omega_n \gg g, \kappa, v, \Omega_n, \tilde{\Omega}_n$.

In analogy to resonator-assisted quantum bath engineering [24], we introduce a rotating transformation \mathbf{R}^n of Pauli operators of each qubit to investigate the polarization efficiency of the arbitrary direction

$$\begin{bmatrix} \sigma_{\mathbf{x}}^n \\ \sigma_{\mathbf{y}}^n \\ \sigma_{\mathbf{z}}^n \end{bmatrix} = \begin{bmatrix} \cos \theta_n \cos \phi_n & -\cos \theta_n \sin \phi_n & \sin \theta_n \\ \sin \phi_n & \cos \phi_n & 0 \\ -\sin \theta_n \cos \phi_n & \sin \theta_n \sin \phi_n & \cos \theta_n \end{bmatrix} \begin{bmatrix} \sigma_x^n \\ \sigma_y^n \\ \sigma_z^n \end{bmatrix} \quad (\text{A.6})$$

with

$$-\frac{\text{Re}(\Omega_n)}{\sin \theta_n \cos \phi_n} = \frac{\text{Im}(\Omega_n)}{\sin \theta_n \sin \phi_n} = \frac{\delta\varpi_n}{2 \cos \theta_n}. \quad (\text{A.7})$$

We can define this ratio as an effective Rabi frequency for each qubit

$$\bar{\Omega} \equiv [|\Omega_n|^2 + |\delta\varpi|^2/4]^{1/2}, \quad (\text{A.8})$$

where we have removed the n -dependence of that by adjusting Ω_n and $\delta\varpi_n$ for simplicity, which is an easy operation in experiment. In rotating frame of $R_2 = H_h + \sum_{n=1}^N \bar{\Omega} \sigma_{\mathbf{z}}^n + \sum_{m=1}^{2N} \delta\omega a_m^+ a_m$, the total Hamiltonian reduces to $H_2(t) = \sum_n H_n(t)$ with

$$\begin{aligned} H_n(t) &= g e^{itR_2} (a_{2n}^+ + a_{2n+1}^+) \sigma_{\mathbf{z}}^n e^{-itR_2} + H.c. \\ &= \left[e^{it\bar{\Omega}\sigma_{\mathbf{z}}^n} (\Theta_{\mathbf{x}}^n \sigma_{\mathbf{x}}^n + \Theta_{\mathbf{y}}^n \sigma_{\mathbf{y}}^n + \Theta_{\mathbf{z}}^n \sigma_{\mathbf{z}}^n) e^{-it\bar{\Omega}\sigma_{\mathbf{z}}^n} \right] \\ &\quad \times g \left[e^{itR_2} (a_{2n}^+ + a_{2n+1}^+) e^{-itR_2} \right] + H.c., \quad (\text{A.9}) \end{aligned}$$

where

$$\Theta_{\mathbf{x}}^n = \frac{1}{2} \cos \theta_n e^{i\phi_n}, \Theta_{\mathbf{y}}^n = -\frac{i}{2} e^{i\phi_n}, \Theta_{\mathbf{z}}^n = \frac{1}{2} \sin \theta_n e^{i\phi_n}. \quad (\text{A.10})$$

Using the Baker-Campbell-Hausdorff expansion, we obtain

$$e^{it\bar{\Omega}\sigma_{\mathbf{z}}^n} \sigma_{\mathbf{x}}^n e^{-it\bar{\Omega}\sigma_{\mathbf{z}}^n} = e^{2it\bar{\Omega}} \sigma_{\mathbf{x}}^n + e^{-2it\bar{\Omega}} \sigma_{\mathbf{x}}^n, \quad (\text{A.11})$$

$$e^{it\bar{\Omega}\sigma_{\mathbf{z}}^n} \sigma_{\mathbf{y}}^n e^{-it\bar{\Omega}\sigma_{\mathbf{z}}^n} = i(e^{-2it\bar{\Omega}} \sigma_{\mathbf{y}}^n - e^{2it\bar{\Omega}} \sigma_{\mathbf{y}}^n), \quad (\text{A.12})$$

$$\begin{aligned} e^{itR_2} a_{2n}^+ e^{-itR_2} &= \frac{1}{2} \left[e^{i(\delta\omega+v)t} a_{2n}^+ + e^{i(\delta\omega-v)t} a_{2n}^+ \right. \\ &\quad \left. + e^{i(\delta\omega+v)t} a_{2n+1}^+ - e^{i(\delta\omega-v)t} a_{2n+1}^+ \right], \quad (\text{A.13}) \end{aligned}$$

$$\begin{aligned} e^{itR_2} a_{2n+1}^+ e^{-itR_2} &= \frac{1}{2} \left[e^{i(\delta\omega+v)t} a_{2n}^+ - e^{i(\delta\omega-v)t} a_{2n}^+ \right. \\ &\quad \left. + e^{i(\delta\omega+v)t} a_{2n+1}^+ + e^{i(\delta\omega-v)t} a_{2n+1}^+ \right], \quad (\text{A.14}) \end{aligned}$$

where $\sigma_{\pm}^{n(\mathbf{z})} = (\sigma_{\mathbf{x}}^n \pm i\sigma_{\mathbf{y}}^n)/2$ are the ladder operators in the \mathbf{z} -basis. Here we emphasize the special structure of the multi-resonator multi-qubit circuit QED architecture. As shown in Eqs. (A.13, A.14), RWA corresponding to resonators only generates two modes ($\delta\omega \pm v$), which greatly reduces the complexity of analytical derivation of the scheme, and efficiently improve the polarization. Let us make comparisons with other three kinds of network structures. The most general multi-cavity and multi-qubit system is the one at which each qubit is coupled to one cavity, which is directly coupled to its neighboring ones. In this case, the second RWA will generate total $3N$ modes, the resetting efficiency will be greatly reduced, because only small proportion of modes are matched. In comparison with the case where qubits interact through $n(n > 2)$ resonators, the second RWA will generate total $3n$ modes. The resetting processes is also influenced by the same reason. The simpler network, where qubits interact through only one resonator, seems to be inconvenient for the scalability.

Substituting Eqs. (A.11-A.14) into Hamiltonian (A.9), we can obtain $H_n(t) = \sum_{l=\pm 1} \sum_{k=0,\pm 1} H_{lk}^n(t)$ with

$$H_{lk}^n(t) = \begin{cases} \sum_m A_{mn}^l g \Theta_{\mathbf{z}}^n e^{i\omega_{lk}t} a_m^+ \sigma_{\mathbf{z}}^{n(\mathbf{z})} + H.c., & k=-1; \\ \sum_m A_{mn}^l g \Theta_{\mathbf{z}}^n e^{i\omega_{lk}t} a_m^+ \sigma_{\mathbf{z}}^{n(\mathbf{z})} + H.c., & k=0; \\ \sum_m A_{mn}^l g \Theta_{\mathbf{z}}^n e^{i\omega_{lk}t} a_m^+ \sigma_{\mathbf{z}}^{n(\mathbf{z})} + H.c., & k=+1. \end{cases} \quad (\text{A.15})$$

where the rotating frame of R_2 makes the Hamiltonian generate six modes $M(l, k)$ ($l = \pm 1, k = 0, \pm 1$) with frequencies $\omega_{lk} = \delta\omega + lv + 2k\bar{\Omega}$, coefficients A_{mn}^l are given in FIG. 4(a)-(b) for the case $N = 3$, and (θ_n, ϕ_n) -dependent coefficients are given by $\Theta_{\pm}^n = e^{i\phi_n} (\cos \theta_n \mp 1)/2$ for the n th qubit.

There is no preference in the $\sigma_{\mathbf{z}}^n$ direction for the dynamics of modes $M(\pm, 0)$ at the thermal equilibrium, while those of modes $M(l, \pm 1)$ will drive the qubit to the $\langle \sigma_{\mathbf{z}}^n \rangle = \pm 1$ states, respectively [24, 28]. Therefore, resonator-assisted cooling requires that we should remove the dynamics of $M(l, +1)$ with appropriate RWA. The (θ_n, ϕ_n) -dependent coefficients Θ_{\pm}^n indicate that this RWA has more warrant for an around- z -axis polarization, where coefficients Θ_{\pm}^n approaches zero and the dynamics of $M(l, +1)$ disappears.

We may set $\Delta_l = \delta\omega + lv - 2\bar{\Omega}$ to be close to zero, and choose the appropriate filter-filter coupling and the effective Rabi frequency, so that other high-frequency modes $M(l', n)$ ($l' \neq l$ or $n \neq -1$) well separate from mode $M(l, -1)$. It happens when $2\bar{\Omega}$ and v are big enough, i.e., $2\bar{\Omega}, v \gg \Delta_l$. In the interaction frame of R_2 , RWA reduces the Hamiltonian into $H_I^l = \sum_{n=1}^N \sum_{m=1}^{2N+2} H_{mn}^l(t)$ with

$$H_{mn}^l(t) = \Theta_{mn}^l a_m^+ \sigma_{\mathbf{z}}^{ln}(t) + \Theta_{mn}^{l*} a_m \sigma_{\mathbf{z}}^{ln}(t), \quad (\text{A.16})$$

where

$$\Theta_{mn}^{\pm} = g A_{mn}^l \Theta_{\pm}^n, \sigma_{\pm}^{ln}(t) = \sigma_{\pm}^{n(\mathbf{z})} e^{\mp i\Delta_l t}. \quad (\text{A.17})$$

This RWA is valid in the parameter regime $2\bar{\Omega}, v \gg \kappa, g$.

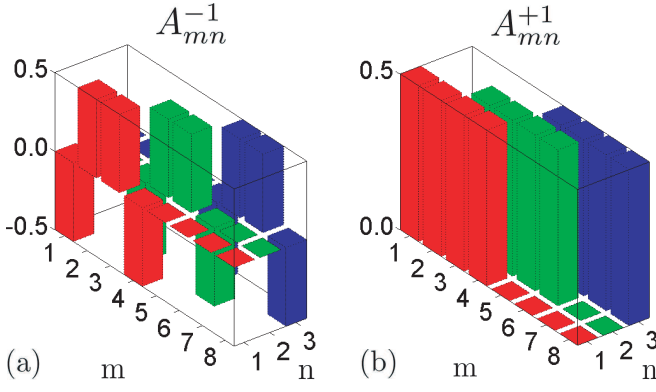


FIG. 4: (a)-(b) The constants A_{mn}^l specified in Eq. (A.15) versus the qubit indices n and the resonator indices m for the system dominated by the mode $M(l, -1)$ (a) $l = -1$ or (b) $l = 0$. Here N is assumed to be 3.

B. Derivation of Markovian master equation

The evolution of the multi-resonator multi-qubit network for the superconducting circuit in an open environment can be modeled by the Lindblad master equation [40],

$$\frac{d}{dt}\rho(t) = L[H_I^l(t)]\rho + D_c\rho(t), \quad (\text{B.1})$$

where index $l = \pm 1$ corresponds to system dominated by mode $M(l, -1)$, $L[H_I^l(t)]\rho = -i[H_I^l(t), \rho]$ is a superoperator describing the unitary evolution under the domination of H_I^l , D_c is a dissipator describing the non-Hermitian dynamics of the system due to the coupling to environment

$$D_c = \sum_{m=1}^{2N+2} \frac{\kappa}{2} ((1 + \bar{n}_m)D[a_m] + \bar{n}_m D[a_m^\dagger]), \quad (\text{B.2})$$

where $D[O]\rho = 2O\rho O^\dagger - \{O^\dagger O, \rho\}$, $\bar{n}_m = \text{tr}_c[a_m^\dagger a_m \rho_{eq}] = 1/(e^{\omega_c/k_B T_c} - 1)$ is the expectation value of the photon number operator at equilibrium associated with the temperature of the bath, T_c , and the Boltzmann constant k_B .

The interaction superoperator can be expressed as $\tilde{Q}(t) = e^{-D_c t} Q(t) e^{D_c t}$ provided it works in the rotating frame with the dissipator D_c , and the system state evolves according to $\tilde{\rho}(t) = e^{-D_c t} \rho(t)$. Then the master equation (B.1) of the whole system reduces to

$$\dot{\tilde{\rho}}(t) = \tilde{L}[H_I^l(t)]\tilde{\rho}(t). \quad (\text{B.3})$$

Let's introduce a projection operator \hat{P} as to satisfy:

$$\hat{P}\rho(t) = \varrho(t) \otimes \rho_{eq}. \quad (\text{B.4})$$

where $\varrho(t) = \text{tr}_c[\rho(t)]$ is the reduced state of N flux-tunable transmon qubits and ρ_{eq} is the resonators equilibrium state. The reduced dynamics of the flux-tunable

transmon qubits are transformed into the 2nd order time-convolutionless (TCL) master equation [40]

$$\frac{d}{dt}\hat{P}\tilde{\rho}(t) = \int_0^t d\tau \hat{P}\tilde{L}[H_I^l(t)]\tilde{L}[H_I^l(t-\tau)]\hat{P}\tilde{\rho}(t). \quad (\text{B.5})$$

Using the algebraic transformation of the dissipator D_c : $\text{tr}_c[D_c^+[O]O'] = \text{tr}_c[OD_c[O']]$ for the arbitrary resonator operator O (O'), and combining the properties:

$$D_c^+[\mathbf{I}] = \mathbf{0}, e^{D_c^+ t}[\mathbf{I}] = \mathbf{1}, \quad (\text{B.6})$$

$$D_c^+[a_m] = -\frac{\kappa}{2}a_m, e^{D_c^+ t}[a_m] = e^{-\kappa t/2}a_m, \quad (\text{B.7})$$

$$D_c^+[a_m^\dagger] = -\frac{\kappa}{2}a_m^\dagger, e^{D_c^+ t}[a_m^\dagger] = e^{-\kappa t/2}a_m^\dagger. \quad (\text{B.8})$$

we have

$$\begin{aligned} \hat{P}\tilde{\rho}(t) &= \text{tr}_c[e^{tD_c} \rho(t)] \otimes \rho_{eq} \\ &= \text{tr}_c[e^{-D_c^+ t} \rho(t)] \otimes \rho_{eq} \\ &= \hat{P}\rho(t). \end{aligned} \quad (\text{B.9})$$

Then the reduced dynamics of the composite system is [28]

$$\begin{aligned} \dot{\varrho}(t) &= \int_0^t d\tau \text{tr}_c[L[H_I^l(t)]e^{D_c \tau} L[H_I^l(t-\tau)]\varrho(t) \otimes \rho_{eq}] \\ &= \int_0^t d\tau \text{tr}_c[e^{D_c^+ \tau} (L[H_I^l(t)])L[H_I^l(t-\tau)]\varrho(t) \otimes \rho_{eq}] \\ &= \int_0^t d\tau e^{-\kappa \tau/2} \text{tr}_c[L[H_I^l(t)]L[H_I^l(t-\tau)]\varrho(t) \otimes \rho_{eq}] \\ &= - \int_0^t d\tau e^{-\kappa \tau/2} \text{tr}_c[[H_I^l(t), [H_I^l(t-\tau), \varrho(t) \otimes \rho_{eq}]]]. \end{aligned} \quad (\text{B.10})$$

With the Definition

$$F_{\vec{n}\vec{i}}^l(t, s) = \text{tr}_c[[H_{in}^l(t), H_{i'n'}^l(s)]\varrho(t) \otimes \rho_{eq}], \quad (\text{B.11})$$

where $\vec{n} = (n, n')$ and $\vec{i} = (i, i')$, the 2nd order TCL master equation (B.10) becomes

$$\dot{\varrho}(t) = - \sum_{\vec{n}, \vec{i}} \int_0^t d\tau e^{-\kappa \tau/2} F_{\vec{n}\vec{i}}^l(t, t-\tau). \quad (\text{B.12})$$

Employing the following equation relation of the resonators equilibrium state

$$\text{tr}_c[a_i a_{i'}^\dagger \rho_{eq}] = (\bar{n}_i + 1)\delta_{i, i'}, \quad (\text{B.13})$$

$$\text{tr}_c[a_i^\dagger a_{i'} \rho_{eq}] = \bar{n}_i \delta_{i, i'}, \quad (\text{B.14})$$

$$\text{tr}_c[a_i^\dagger a_{i'}^\dagger \rho_{eq}] = 0, \quad (\text{B.15})$$

$$\text{tr}_c[a_i a_{i'} \rho_{eq}] = 0, \quad (\text{B.16})$$

we obtain

$$\begin{aligned}
F_{\vec{n}\vec{i}}^l(t, s) &= \text{tr}_c[\Theta_{in}^l a_i^+ \sigma_-^{ln}(t), [\Theta_{i'n'}^{l*} a_{i'} \sigma_+^{ln'}(s), \varrho(t) \otimes \rho_{eq}]] + \text{tr}_c[\Theta_{in}^{l*} a_i \sigma_+^{ln}(t), [\Theta_{i'n'}^l a_{i'}^+ \sigma_-^{ln'}(s), \varrho(t) \otimes \rho_{eq}]] \\
&= \Theta_{in}^l \Theta_{i'n'}^{l*} \left\{ \text{tr}_c[a_i^+ a_{i'} \rho_{eq}][\sigma_-^{ln}(t) \sigma_+^{ln'}(s) \varrho - \sigma_-^{ln}(t) \varrho \sigma_+^{ln'}(s)] + \text{tr}_c[a_{i'} a_i^+ \rho_{eq}][\varrho \sigma_+^{ln'}(s) \sigma_-^{ln}(t) - \sigma_+^{ln'}(s) \varrho \sigma_-^{ln}(t)] \right\} \\
&+ \Theta_{in}^{l*} \Theta_{i'n'}^l \left\{ \text{tr}_c[a_{i'}^+ a_i \rho_{eq}][\varrho \sigma_-^{ln'}(s) \sigma_+^{ln}(t) - \sigma_-^{ln'}(s) \varrho \sigma_+^{ln}(t)] + \text{tr}_c[a_i a_{i'}^+ \rho_{eq}][\sigma_+^{ln}(t) \sigma_-^{ln'}(s) \varrho - \sigma_+^{ln}(t) \varrho \sigma_-^{ln'}(s)] \right\} \\
&= \delta_{i,i'} \left\{ \Theta_{in}^l \Theta_{in'}^{l*} \bar{n}_i [\sigma_-^{ln}(t) \sigma_+^{ln'}(s) \varrho - \sigma_-^{ln}(t) \varrho \sigma_+^{ln'}(s)] + \Theta_{in}^{l*} \Theta_{in'}^l \bar{n}_i [\varrho \sigma_-^{ln'}(s) \sigma_+^{ln}(t) - \sigma_-^{ln'}(s) \varrho \sigma_+^{ln}(t)] \right. \\
&+ \left. \Theta_{in}^l \Theta_{in'}^{l*} (\bar{n}_i + 1) [\varrho \sigma_+^{ln'}(s) \sigma_-^{ln}(t) - \sigma_+^{ln'}(s) \varrho \sigma_-^{ln}(t)] + \Theta_{in}^{l*} \Theta_{in'}^l (\bar{n}_i + 1) [\sigma_+^{ln}(t) \sigma_-^{ln'}(s) \varrho - \sigma_+^{ln}(t) \varrho \sigma_-^{ln'}(s)] \right\} \quad (\text{B.17})
\end{aligned}$$

Let's set the upper limit of the integral to infinity: $\int_0^t d\tau \rightarrow \int_0^\infty d\tau$ and introduce the superoperator generators

$$G_{\vec{n}\vec{i}}^l(t) \varrho(t) = - \int_0^\infty d\tau e^{-\kappa\tau/2} F_{\vec{n}\vec{i}}^l(t, t - \tau), \quad (\text{B.18})$$

in order to reduce the master equation to

$$\frac{d}{dt} \varrho(t) = \sum_{\vec{n}, \vec{i}} G_{\vec{n}\vec{i}}^l(t) \varrho(t). \quad (\text{B.19})$$

Using the following formula of integration

$$\int_0^\infty d\tau e^{-\kappa\tau/2} e^{\pm i\tau\Delta_l} = \frac{2}{\kappa \mp i2\Delta_l} = \eta_l \pm i\lambda_l, \quad (\text{B.20})$$

with

$$\eta_l = \frac{2\kappa}{\kappa^2 + 4\Delta_l^2}, \lambda_l = \frac{4\Delta_l}{\kappa^2 + 4\Delta_l^2}, \quad (\text{B.21})$$

we have

$$\begin{aligned}
G_{\vec{n}\vec{i}}^l(t) \varrho(t) &= - \int_0^\infty d\tau e^{-\kappa\tau/2} F_{\vec{n}\vec{i}}^l(t, t - \tau) \\
&= -\delta_{i,i'} \int_0^\infty d\tau e^{-\kappa\tau/2} \left\{ e^{i\Delta_l\tau} \Theta_{in}^l \Theta_{in'}^{l*} \bar{n}_i [\sigma_-^{ln} \sigma_+^{ln'} \varrho - \sigma_-^{ln} \varrho \sigma_+^{ln'}] + e^{-i\Delta_l\tau} \Theta_{in}^{l*} \Theta_{in'}^l \bar{n}_i [\varrho \sigma_-^{ln'} \sigma_+^{ln} - \sigma_-^{ln'} \varrho \sigma_+^{ln}] \right. \\
&+ \left. e^{i\Delta_l\tau} \Theta_{in}^l \Theta_{in'}^{l*} (\bar{n}_i + 1) [\varrho \sigma_+^{ln'} \sigma_-^{ln} - \sigma_+^{ln'} \varrho \sigma_-^{ln}] + e^{-i\Delta_l\tau} \Theta_{in}^{l*} \Theta_{in'}^l (\bar{n}_i + 1) [\sigma_+^{ln} \sigma_-^{ln'} \varrho - \sigma_+^{ln} \varrho \sigma_-^{ln'}] \right\}, \\
&= -\delta_{i,i'} \left\{ (\eta_l + i\lambda_l) \Theta_{in}^l \Theta_{in'}^{l*} \bar{n}_i [\sigma_-^{ln} \sigma_+^{ln'} \varrho - \sigma_-^{ln} \varrho \sigma_+^{ln'}] + (\eta_l - i\lambda_l) \Theta_{in}^{l*} \Theta_{in'}^l \bar{n}_i [\varrho \sigma_-^{ln'} \sigma_+^{ln} - \sigma_-^{ln'} \varrho \sigma_+^{ln}] \right. \\
&+ (\eta_l + i\lambda_l) \Theta_{in}^l \Theta_{in'}^{l*} (\bar{n}_i + 1) [\varrho \sigma_+^{ln'} \sigma_-^{ln} - \sigma_+^{ln'} \varrho \sigma_-^{ln}] + (\eta_l - i\lambda_l) \Theta_{in}^{l*} \Theta_{in'}^l (\bar{n}_i + 1) [\sigma_+^{ln} \sigma_-^{ln'} \varrho - \sigma_+^{ln} \varrho \sigma_-^{ln'}] \left. \right\}, \\
&= -\delta_{i,i'} \left\{ \bar{n}_i \eta_l [\Theta_{in}^l \Theta_{in'}^{l*} (\sigma_-^{ln} \sigma_+^{ln'} \varrho - \sigma_-^{ln} \varrho \sigma_+^{ln'}) + \Theta_{in}^{l*} \Theta_{in'}^l (\varrho \sigma_-^{ln'} \sigma_+^{ln} - \sigma_-^{ln'} \varrho \sigma_+^{ln})] \right. \\
&+ i\bar{n}_i \lambda_l [\Theta_{in}^l \Theta_{in'}^{l*} (\sigma_-^{ln} \sigma_+^{ln'} \varrho - \sigma_-^{ln} \varrho \sigma_+^{ln'}) - \Theta_{in}^{l*} \Theta_{in'}^l (\varrho \sigma_-^{ln'} \sigma_+^{ln} - \sigma_-^{ln'} \varrho \sigma_+^{ln})] \\
&+ (\bar{n}_i + 1) \eta_l [\Theta_{in}^l \Theta_{in'}^{l*} (\varrho \sigma_+^{ln'} \sigma_-^{ln} - \sigma_+^{ln'} \varrho \sigma_-^{ln}) + \Theta_{in}^{l*} \Theta_{in'}^l (\sigma_+^{ln} \sigma_-^{ln'} \varrho - \sigma_+^{ln} \varrho \sigma_-^{ln'})] \\
&+ \left. i(\bar{n}_i + 1) \lambda_l [\Theta_{in}^l \Theta_{in'}^{l*} (\varrho \sigma_+^{ln'} \sigma_-^{ln} - \sigma_+^{ln'} \varrho \sigma_-^{ln}) - \Theta_{in}^{l*} \Theta_{in'}^l (\sigma_+^{ln} \sigma_-^{ln'} \varrho - \sigma_+^{ln} \varrho \sigma_-^{ln'})] \right\}. \quad (\text{B.22})
\end{aligned}$$

In view of the identity of N separated qubits, we only discuss the evolution of one qubit, the state of that is diagonal in the coupled angular momentum basis $\varrho^n(t) = \sum_{i=\pm 1} P_i(t) \varrho_i^n$. Here we finally consider the diagonal matrix elements $P_{\sigma_{\mathbf{z}}^n}(t) = \langle \sigma_{\mathbf{z}}^n | \varrho^n(t) | \sigma_{\mathbf{z}}^n \rangle$ ($\sigma_{\mathbf{z}}^n = \pm 1$) of the reduced density operator $\varrho^n(t)$, which corresponds to the expectation value of the projection operator $\varrho_{\sigma_{\mathbf{z}}^n}^n = |\sigma_{\mathbf{z}}^n\rangle \langle \sigma_{\mathbf{z}}^n|$ at an arbitrary time t . For the ath qubit, we obtain

$$\begin{aligned}
\frac{d}{dt}P_{\sigma_z^a}(t) &= \sum_{\vec{n}, \vec{i}} \text{tr}_a[G_{\vec{n}\vec{i}}^l(t)\varrho(t)\varrho_{\sigma_z^a}] \\
&= - \sum_{nn'} \sum_i \left\{ \bar{n}_i \eta_l \text{tr}_a[\Theta_{in}^l \Theta_{in'}^{l*}(\sigma_-^n \sigma_+^{n'} \varrho_{\sigma_z^a} - \sigma_-^n \varrho_{\sigma_z^a} \sigma_+^{n'}) + \Theta_{in}^{l*} \Theta_{in'}^l(\varrho_{\sigma_z^a} \sigma_-^n \sigma_+^{n'} - \sigma_-^{n'} \varrho_{\sigma_z^a} \sigma_+^n)] \right. \\
&\quad + i\bar{n}_i \lambda_l \text{tr}_a[\Theta_{in}^l \Theta_{in'}^{l*}(\sigma_-^n \sigma_+^{n'} \varrho_{\sigma_z^a} - \sigma_-^n \varrho_{\sigma_z^a} \sigma_+^{n'}) - \Theta_{in}^{l*} \Theta_{in'}^l(\varrho_{\sigma_z^a} \sigma_-^n \sigma_+^{n'} - \sigma_-^{n'} \varrho_{\sigma_z^a} \sigma_+^n)] \\
&\quad + (\bar{n}_i + 1) \eta_l \text{tr}_a[\Theta_{in}^l \Theta_{in'}^{l*}(\varrho_{\sigma_z^a} \sigma_-^n \sigma_+^{n'} - \sigma_-^{n'} \varrho_{\sigma_z^a} \sigma_+^n) + \Theta_{in}^{l*} \Theta_{in'}^l(\sigma_+^n \sigma_-^{n'} \varrho_{\sigma_z^a} - \sigma_+^{n'} \varrho_{\sigma_z^a} \sigma_-^n)] \\
&\quad \left. + i(\bar{n}_i + 1) \lambda_l \text{tr}_a[\Theta_{in}^l \Theta_{in'}^{l*}(\varrho_{\sigma_z^a} \sigma_-^n \sigma_+^{n'} - \sigma_-^{n'} \varrho_{\sigma_z^a} \sigma_+^n) - \Theta_{in}^{l*} \Theta_{in'}^l(\sigma_+^n \sigma_-^{n'} \varrho_{\sigma_z^a} - \sigma_+^{n'} \varrho_{\sigma_z^a} \sigma_-^n)] \right\} \\
&= - \sum_{nn'} \sum_i \left\{ \bar{n}_i \eta_l \text{tr}_a[\Theta_{in}^l \Theta_{in'}^{l*}(\varrho_{\sigma_z^a} \sigma_-^n \sigma_+^{n'} - \varrho_{\sigma_z^a} \sigma_+^{n'} \sigma_-^n) + \Theta_{in}^{l*} \Theta_{in'}^l(\varrho_{\sigma_z^a} \sigma_-^n \sigma_+^{n'} - \varrho_{\sigma_z^a} \sigma_+^{n'} \sigma_-^n)] \right. \\
&\quad + i\bar{n}_i \lambda_l \text{tr}_a[\Theta_{in}^l \Theta_{in'}^{l*}(\varrho_{\sigma_z^a} \sigma_-^n \sigma_+^{n'} - \varrho_{\sigma_z^a} \sigma_+^{n'} \sigma_-^n) - \Theta_{in}^{l*} \Theta_{in'}^l(\varrho_{\sigma_z^a} \sigma_-^n \sigma_+^{n'} - \varrho_{\sigma_z^a} \sigma_+^{n'} \sigma_-^n)] \\
&\quad + (\bar{n}_i + 1) \eta_l \text{tr}_a[\Theta_{in}^l \Theta_{in'}^{l*}(\varrho_{\sigma_z^a} \sigma_+^n \sigma_-^{n'} - \varrho_{\sigma_z^a} \sigma_-^{n'} \sigma_+^n) + \Theta_{in}^{l*} \Theta_{in'}^l(\varrho_{\sigma_z^a} \sigma_+^n \sigma_-^{n'} - \varrho_{\sigma_z^a} \sigma_-^{n'} \sigma_+^n)] \\
&\quad \left. + i(\bar{n}_i + 1) \lambda_l \text{tr}_a[\Theta_{in}^l \Theta_{in'}^{l*}(\varrho_{\sigma_z^a} \sigma_+^n \sigma_-^{n'} - \varrho_{\sigma_z^a} \sigma_-^{n'} \sigma_+^n) - \Theta_{in}^{l*} \Theta_{in'}^l(\varrho_{\sigma_z^a} \sigma_+^n \sigma_-^{n'} - \varrho_{\sigma_z^a} \sigma_-^{n'} \sigma_+^n)] \right\} \\
&= - \sum_i |\Theta_{ia}^l|^2 \left\{ \bar{n}_i \eta_l \text{tr}_a[(\varrho_{\sigma_z^a} \sigma_-^a \sigma_+^a - \varrho_{\sigma_z^a} \sigma_+^a \sigma_-^a) + (\varrho_{\sigma_z^a} \sigma_+^a \sigma_-^a - \varrho_{\sigma_z^a} \sigma_-^a \sigma_+^a)] \right. \\
&\quad + i\bar{n}_i \lambda_l \text{tr}_a[(\varrho_{\sigma_z^a} \sigma_-^a \sigma_+^a - \varrho_{\sigma_z^a} \sigma_+^a \sigma_-^a) - (\varrho_{\sigma_z^a} \sigma_+^a \sigma_-^a - \varrho_{\sigma_z^a} \sigma_-^a \sigma_+^a)] \\
&\quad + (\bar{n}_i + 1) \eta_l \text{tr}_a[(\varrho_{\sigma_z^a} \sigma_+^a \sigma_-^a - \varrho_{\sigma_z^a} \sigma_-^a \sigma_+^a) + (\varrho_{\sigma_z^a} \sigma_+^a \sigma_-^a - \varrho_{\sigma_z^a} \sigma_-^a \sigma_+^a)] \\
&\quad \left. + i(\bar{n}_i + 1) \lambda_l \text{tr}_a[(\varrho_{\sigma_z^a} \sigma_+^a \sigma_-^a - \varrho_{\sigma_z^a} \sigma_-^a \sigma_+^a) - (\varrho_{\sigma_z^a} \sigma_+^a \sigma_-^a - \varrho_{\sigma_z^a} \sigma_-^a \sigma_+^a)] \right\} \\
&= - \sum_i \eta_l |\Theta_{ia}^l|^2 \left\{ 2\bar{n}_i [P_{\sigma_z^a}(t)\Lambda_{\sigma_z^a}^+ - P_{\sigma_z^a-1}(t)\Lambda_{\sigma_z^a}^-] \right. \\
&\quad \left. + 2(\bar{n}_i + 1)[P_{\sigma_z^a}(t)\Lambda_{\sigma_z^a}^- - P_{\sigma_z^a+1}(t)\Lambda_{\sigma_z^a}^+] \right\}, \tag{B.23}
\end{aligned}$$

with $\Lambda_{\beta 1}^a = \delta_{a,-\beta}$.

With the definition of $\vec{P}_{\sigma_z^n}(t) = (P_{-1}(t), P_1(t))^T$, the master equation (B.23) reduces to a rate equation for the state populations:

$$\frac{d}{dt}\vec{P}_{\sigma_z^n}(t) = \Gamma_n^l \mathbf{M} \vec{P}_{\sigma_z^n}(t), \tag{B.24}$$

with

$$\mathbf{M} = \begin{bmatrix} -\bar{n} & \bar{n} + 1 \\ \bar{n} & -(\bar{n} + 1) \end{bmatrix}, \tag{B.25}$$

$$\Gamma_n^l = \sum_i 2\eta_l |\Theta_{in}^l|^2. \tag{B.26}$$

Substituting (A.17) and (B.21) into (B.26), we obtain the effective dissipation rate of each qubit for different dominated modes $M(l, -1)$

$$\Gamma_n^l = \frac{(1 + \cos \theta_n)^2}{1 + 4(\Delta/\kappa)^2} \frac{g^2}{\kappa}. \tag{B.27}$$

-
- [1] M. A. Nielsen, and I. L. Chuang, *Quantum computation and quantum information* (Cambridge Univ. Press, 2010).
 - [2] N. D. Mermin, *Quantum Computer Science* (Cambridge Univ. Press, 2007).
 - [3] M. J. Hartmann, F. G. Brandao, and M. B. Plenio, *Quantum many-body phenomena in coupled cavity arrays*, *Laser and Photonics Reviews* **2**, 527 (2008).
 - [4] J. I. Cirac, and P. Zoller, *Goals and opportunities in*

- quantum simulation*, *Nature Physics* **8**, 264 (2012).
- [5] I. Bloch, J. Dalibard, and S. Nascimbène, *Quantum simulations with ultracold quantum gases*, *Nature Physics* **8**, 267 (2012).
- [6] H. J. Kimble, *The quantum internet*, *Nature* **453**, 1023 (2008).
- [7] C. W. Chou, J. Laurat, H. Deng, K. S. Choi, H. Riedmaten, D. Felinto, and H. J. Kimble, *Functional quantum nodes for entanglement distribution over scalable quan-*

- tum networks*, Science **316**, 1316 (2007).
- [8] H. Ritsch, P. Domokos, F. Brennecke, and T. Esslinger, *Cold atoms in cavity-generated dynamical optical potentials*, Rev. Mod. Phys. **85**, 553 (2013).
 - [9] Z.-L. Xiang, S. Ashhab, J. Q. You, and F. Nori, *Hybrid quantum circuits: Superconducting circuits interacting with other quantum systems*, Rev. Mod. Phys. **85**, 623 (2013).
 - [10] M. H. Devoret, and R. J. Schoelkopf, *Superconducting circuits for quantum information: an outlook*, Science **339**, 1169 (2013).
 - [11] D. P. DiVincenzo, *The Physical Implementation of Quantum Computation*, Fortschar. Phys. **48**, 771 (2000).
 - [12] P. Schindler, J. T. Barreiro, T. Monz, V. Nebendahl, D. Nigg, M. Chwalla, M. Hennrich, and R. Blatt, *Experimental repetitive quantum error correction*, Science **332**, 1059 (2011).
 - [13] M. D. Reed, L. DiCarlo, S. E. Nigg, L. Sun, L. Frunzio, S. M. Girvin, and R. J. Schoelkopf, *Realization of three-qubit quantum error correction with superconducting circuits*, Nature **482**, 382 (2012).
 - [14] J. J. L. Morton, A. M. Tyryshkin, R. M. Brown, S. Shankar, B. W. Lovett, A. Ardavan, T. Schenkel, E. E. Haller, J. W. Ager, and S. A. Lyon, *Solid state quantum memory using the ^{31}P nuclear spin*, Nature **455**, 1085 (2008).
 - [15] D. I. Schuster, A. P. Sears, E. Ginossar, L. DiCarlo, L. Frunzio, J. J. L. Morton, H. Wu, G. A. D. Briggs, B. B. Buckley, D. D. Awschalom, and R. J. Schoelkopf, *High-cooperativity coupling of electron-spin ensembles to superconducting cavities*, Phys. Rev. Lett. **105**, 140501 (2010).
 - [16] Y. Kubo, F. R. Ong, P. Bertet, D. Vion, V. Jacques, D. Zheng, A. Dreau, J. F. Roch, A. Auffeves, F. Jelezko, J. Wrachtrup, M. F. Barthe, P. Bergonzo, and D. Esteve, *Strong coupling of a spin ensemble to a superconducting resonator*, Phys. Rev. Lett. **105**, 140502 (2010).
 - [17] I. Chiorescu, N. Groll, S. Bertaina, T. Mori, and S. Miyashita, *Magnetic strong coupling in a spin-photon system and transition to classical regime*, Phys. Rev. B **82**, 024413 (2010).
 - [18] J. F. Poyatos, J. I. Cirac, and P. Zoller, *Quantum reservoir engineering with laser cooled trapped ions*, Phys. Rev. Lett. **77**, 4728 (1996).
 - [19] B. Kraus, H. P. Buchler, S. Diehl, A. Kantian, A. Micheli, and P. Zoller, *Preparation of entangled states by quantum Markov processes*, Phys. Rev. A **78**, 042307 (2008).
 - [20] D. Marcos, V. Tomadin, S. Diehl, and P. Rabl, *Photon condensation in circuit quantum electrodynamics by engineered dissipation*, New J. Phys. **14**, 055005 (2012).
 - [21] M. D. Reed, B. R. Johnson, A. A. Houck, L. DiCarlo, J. M. Chow, D. I. Schuster, L. Frunzio, and R. J. Schoelkopf, *Fast reset and suppressing spontaneous emission of a superconducting qubit*, App. Phys. Lett. **96**, 203110 (2010).
 - [22] K. W. Murch, U. Vool, D. Zhou, S. J. Weber, S. M. Girvin, and I. Siddiqi, *Cavity-assisted quantum bath engineering*, Phys. Rev. Lett. **109**, 183602 (2012).
 - [23] K. Geerlings, Z. Leghtas, I. M. Pop, S. Shankar, L. Frunzio, R. J. Schoelkopf, M. Mirrahimi, and M. H. Devoret, *Demonstrating a driven reset protocol for a superconducting qubit*, Phys. Rev. Lett. **110**, 120501 (2013).
 - [24] X. P. Zhang, L. T. Shen, Z. Q. Yin, H. Z. Wu, and Z. B. Yang, *Resonator-assisted quantum bath engineering of a flux qubit*, Phys. Rev. A **91**, 013825 (2015).
 - [25] P. Maunz, T. Puppe, I. Schuster, N. Syassen, P.W. H. Pinkse, and G. Rempe, *Cavity cooling of a single atom*, Nature (London) **428**, 50 (2004).
 - [26] D. R. Leibbrandt, J. Labaziewicz, V. Vuletic, and I. L. Chuang, *Cavity sideband cooling of a single trapped ion*, Phys. Rev. Lett. **103**, 103001 (2009).
 - [27] N. Brahms and D. M. Stamper-Kurn, *Spin optodynamics analog of cavity optomechanics*, Phys. Rev. A **82**, 041804 (2010).
 - [28] C. J. Wood, T. W. Borneman, and D. G. Cory, *Cavity cooling of an ensemble spin system*, Phys. Rev. Lett. **112**, 050501 (2014).
 - [29] O. Arcizet, P.-F. Cohadon, T. Briant, M. Pinard, and A. Heidmann, *Radiation-pressure cooling and optomechanical instability of a micromirror*, Nature (London) **444**, 71 (2006).
 - [30] S. Gigan, H. R. Böhm, M. Paternostro, F. Blaser, G. Langer, J. B. Hertzberg, K. C. Schwab, D. Bäuerle, M. Aspelmeyer, and A. Zeilinger, *Self-cooling of a micromirror by radiation pressure*, Nature (London) **444**, 67 (2006).
 - [31] A. Naik, O. Buu, M. D. LaHaye, A. D. Armour, A. A. Clerk, M. P. Blencowe, and K. C. Schwab, *Cooling a nanomechanical resonator with quantum back-action*, Nature (London) **443**, 193 (2006).
 - [32] J.-L. Orgiazzi, C. Deng, D. Layden, R. Marchildon, F. Kitapli, F. Shen, M. Bal, F. R. Ong, and A. Lupascu, *Flux qubits in a planar circuit quantum electrodynamics architecture: quantum control and decoherence*, arXiv:1407.1346v1.
 - [33] M. Stern, G. Catelani, Y. Kubo, C. Grezes, A. Bienfait, D. Vion, D. Esteve, and P. Bertet, *Flux qubits with long coherence times for hybrid quantum circuits*, Phys. Rev. Lett. **113**, 123601 (2014).
 - [34] H. Paik, D. I. Schuster, Lev S. Bishop, G. Kirchmair, G. Catelani, A. P. Sears, B. R. Johnson, M. J. Reagor, L. Frunzio, L. I. Glazman, S. M. Girvin, M. H. Devoret, and R. J. Schoelkopf, *Observation of high coherence in Josephson junction qubits measured in a three-dimensional circuit QED architecture*, Phys. Rev. Lett. **107**, 240501 (2011).
 - [35] A. A. Houck, J. A. Schreier, B. R. Johnson, J. M. Chow, J. Koch, J. M. Gambetta, D. I. Schuster, L. Frunzio, M. H. Devoret, S. M. Girvin and R. J. Schoelkopf, *Controlling the Spontaneous Emission of a Superconducting Transmon Qubit*, Phys. Rev. Lett. **101**, 080502 (2008).
 - [36] D. C. McKay, R. Naik, P. Reinhold, Lev S. Bishop, and D. I. Schuster, *High-Contrast Qubit Interactions Using Multimode Cavity QED*, Phys. Rev. Lett. **114**, 080501 (2015).
 - [37] The mode $M(-1, 1)$ almost has the same frequency as mode $M(1, -1)$ when filter-filter coupling v approaches $2\bar{\Omega}$. In such a case, the competition of modes $M(-1, 1)$ and $M(1, -1)$ will produce a severe disturbance on the polarization process.
 - [38] J. R. Johansson, P. D. Nationa, and Franco Noria, *QuTiP: An open-source Python framework for the dynamics of open quantum systems*, Comp. Phys. Comm. **183**, 1760 (2012).
 - [39] J. R. Johansson, P. D. Nationa, and Franco Noria, *QuTiP 2: A Python framework for the dynamics of open quantum systems*, Comp. Phys. Comm. **184**, 1234 (2013).
 - [40] H.-P. Breuer and F. Petruccione, *The Theory of Open Quantum Systems* (Oxford University Press, New York,

- 2002).
- [41] G. S. Agarwal, *Quantum Optics* (Springer-Verlag, Berlin, 1974).